# Characterization of Semiconductor-Based Optical Frequency Comb Sources Using Generalized Multiheterodyne Detection

Anthony Klee, *Student Member, IEEE*, Josue Davila-Rodriguez, *Student Member, IEEE*, Charles Williams, *Student Member, IEEE*, and Peter J. Delfyett, *Fellow, IEEE*

*(Invited Paper)*

***Abstract*—A spectrally efficient multiheterodyne scheme is applied for the independent measurement of the spectral phase profiles of three distinct semiconductor frequency combs. The amount of quadratic and cubic phase is quantified for each source, providing insight on the dispersive properties of the semiconductor gain and the fiberized laser cavity. This information is vital for the optimization and expansion of the spectral bandwidth of such sources.**

***Index Terms*—Multiheterodyne spectroscopy, optical frequency combs, semiconductor mode-locked lasers (MLLs).**

## I. Introduction

OPTICAL frequency comb sources have garnered much attention due to their extreme stability and purity in the optical frequency spectrum, with spectral coherence spanning up to hundreds of terahertz. Owing to these properties, optical frequency combs have found applications in precision metrology [1], time transfer [2], pulse shaping [3], matched filtering [4], and coherent communications and signal processing [4], [5]. Optical frequency combs can be generated in a variety of ways, such as from mode-locked lasers (MLLs) as well as from cascaded nonlinear optical effects in microcavity resonators and optical fibers [6]. The resulting comb quality varies greatly depending on the method of generation. Even in the case of MLLs where one might assume predictable comb quality, comb characteristics can vary drastically depending on the mode-locking mechanism and the comb stabilization scheme.

Several methods exist to characterize the spectral quality of comb sources and MLLs, such as intensity correlation, frequency-resolved optical gating (FROG) [7], and spectral phase interferometry for direct electric field reconstruction (SPIDER) [8]. Correlation methods provide only a qualitative measure of pulse shape, and little information on the temporal or spectral phase characteristics. FROG and SPIDER can provide information about the complete temporal and spectral fields, but rely on nonlinear optical effects and thus become difficult to use for low peak power signals or waveforms with large time-bandwidth products. Multiheterodyne detection has been shown to be an effective phase-sensitive method for the compression and downconversion of optical comb spectra [9], [10]. In multiheterodyne detection, two optical frequency combs with slightly different repetition rates beat to produce a frequency comb in the RF domain [11]. If the two optical frequency combs are frequency stabilized, it is possible to have narrow linewidth beat frequencies that can be individually resolved, allowing for optical phase information to be recovered [12], [13]. However, prior to recent advancements, it has been required that one of the optical frequency combs producing the multiheterodyne signal serves as a reference with flat spectral magnitude and purely linear spectral phase, leading to errors in the recovered spectrum if this requirement was not fulfilled. By considering a larger portion of the photodetected multiheterodyne spectrum and applying a noniterative algorithm, independent measurements of the complex spectra of each comb source can be simultaneously obtained, obviating the need for a perfect reference comb [14]. At the cost of a more complicated algorithm, reducing the repetition rate of one comb source to nearly match a small subharmonic of the second comb's repetition rate decreases how much of the multiheterodyne spectrum must be acquired to perform amplitude and phase retrieval by up to 50% of the higher repetition rate [15]. Multiheterodyne detection can be quite demanding in its requirements on the comb sources and detection electronics, but the retrieval algorithm of [14] and [15] and reduction of necessary RF bandwidth can help to relax these constraints and make it a more accessible technique.

In this paper, we present this generalized retrieval algorithm and apply it to the complete characterization of three different classes of stabilized optical frequency comb sources based on mode-locked semiconductor diode lasers: 1) a harmonically mode-locked diode source that is frequency stabilized using optical injection-locking techniques; 2) a harmonically mode-locked diode laser stabilized using an intracavity etalon as a secondary optical reference; and 3) a harmonically mode-locked diode laser similar to 2, but with dispersion compensation and a different gain medium, providing high intracavity power. Our

Manuscript received November 1, 2012; revised December 17, 2012; accepted December 19, 2012. Date of publication January 4, 2013; date of current version May 13, 2013. This work was supported in part by the National Science Foundation under Contract DMR 0120967.

The authors are with the Center for Research and Education in Optics and Lasers, College of Optics and Photonics, University of Central Florida, Orlando, FL 32816 USA (e-mail: acklee@creol.ucf.edu; josue@creol.ucf.edu; charles@creol.ucf.edu; delfyett@creol.ucf.edu).

Color versions of one or more of the figures in this paper are available online at http://ieeexplore.ieee.org.

Digital Object Identifier 10.1109/JSTQE.2013.2237887

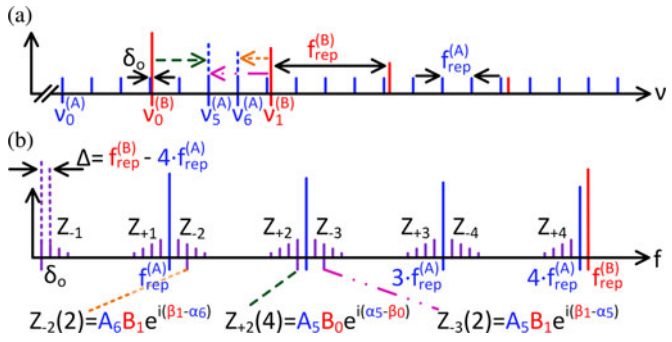


Fig. 1. Multiheterodyne (a) optical spectrum and (b) RF spectrum for $N_H = 4$. Intracomb beats from Combs A to B shown in blue and red, respectively, and intercomb beats are shown in purple. Three intercomb optical combline pairs and their corresponding RF beats are called out to demonstrate the source of various beat sets.

results show that the retrieved spectral phase of each of the three measured diode-based frequency comb source shows salient similarities with key subtle differences. More importantly, the differences can be directly traced back to the underlying properties of the stabilized cavity and the intracavity linear and nonlinear optical properties.

This paper is organized as follows: First, a description of the multiheterodyne-based characterization method is given, highlighting the generalized theory and identifying criteria for the optical and RF spectra to provide a robust multiheterodyne signal. Next, an algorithm for retrieval of the spectral phase is provided, noting the benefits of the general approach, followed by a description of the experimental setup used in these measurement. This paper continues with descriptions of the three classes of stabilized diode comb sources along with the measured spectral intensity and retrieved spectral phase.

## II. Characterization Method

### A. General Multiheterodyne Theory

Consider two optical frequency combs, Combs A and B, with comblines occurring at $\nu_n^{(\mathrm{A,B})} = \nu_o^{(\mathrm{A,B})} + n \cdot f_{\mathrm{rep}}^{(\mathrm{A,B})}$, where $\nu_n$ is the frequency of the $n$th combline, $\nu_o$ is the lowest frequency combline in the lasing spectrum (not to be confused with the carrier-envelope offset frequency), $f_{\mathrm{rep}}$ is the mode spacing or repetition rate, and superscripts refer to the comb source. Let the complex amplitude of the $\nu_n^{(\mathrm{A})}(\nu_n^{(\mathrm{B})})$ combline be given by $\mathrm{A}_n \mathrm{e}^{\mathrm{i}\alpha_n}$ ($\mathrm{B}_n \mathrm{e}^{\mathrm{i}\beta_n}$). Assume that $f_{\mathrm{rep}}^{(\mathrm{A})}$ and $f_{\mathrm{rep}}^{(\mathrm{B})}$ are not equal, nor exact harmonics of each other, and take $f_{\mathrm{rep}}^{(\mathrm{B})}$ to be the larger of the two. If the two combs have overlapping spectra, then the combined optical spectrum consists of interleaved combs where the spacing between comblines from Comb B and the nearest frequency neighbor from Comb A changes across the spectrum, as seen in Fig. 1(a). In general, $f_{\mathrm{rep}}^{(\mathrm{B})}$ may be several times larger than $f_{\mathrm{rep}}^{(\mathrm{A})}$, resulting in multiple comblines from Comb A falling between any two adjacent comblines of Comb B. Here, it is useful to define the subharmonic order, or integer ratio of repetition rates, as $N_H = \left\lfloor f_{\mathrm{rep}}^{(\mathrm{B})} / f_{\mathrm{rep}}^{(\mathrm{A})} \right\rfloor$.

Upon photodetection, the mixing products of the two combs are generated as seen in Fig. 1(b), producing intracomb heterodyne beat tones at $f_{\mathrm{rep}}^{(\mathrm{A})}$, $f_{\mathrm{rep}}^{(\mathrm{B})}$, and their harmonics and intercomb heterodyne beat tones at a multitude of RF frequencies due to the difference in repetition rates. The intercomb beats are spaced by the effective repetition rate detuning $\Delta = f_{\mathrm{rep}}^{(\mathrm{B})} - N_H \cdot f_{\mathrm{rep}}^{(\mathrm{A})}$, with the first beat occurring at $\delta_o$, the frequency difference between the nearest two optical comblines. The magnitude of an individual heterodyne beat is given by the product of the constituent optical combline magnitudes, and the phase given by the optical phase difference; therefore, the complex spectral information of both combs is completely contained in the RF spectrum. However, the intracomb beats are the composite of many pairs of comblines while each of the intercomb beats can be uniquely determined by a single optical pair.

As will be seen in the following treatment, it is vital that each intercomb beat is uniquely determined by a single pair of optical comblines which can be ensured through proper choice of $\nu_{\mathrm{o}}^{(\mathrm{A,B})}$ and $f_{\mathrm{rep}}^{(\mathrm{A,B})}$. To prevent aliasing of the beat tones, which can lead to multiple optical pairs contributing to the same beat frequency, all beats between Comb B comblines and the nearest low frequency neighbor from Comb A must fall below $f_{\mathrm{rep}}^{(\mathrm{A})}/2$, satisfying the condition of (1), where $N_{\mathrm{B}}$ is the number of optical comb lines in Comb B. The number of comblines in Comb B will be less than the number of comblines in Comb A for all cases of interest

$$(N_{\mathrm{B}} - 1)\,\Delta + \delta_o < \frac{f_{\mathrm{rep}}^{(\mathrm{A})}}{2}. \tag{1}$$

If this condition is satisfied, then it can be seen that the RF beat tones group into sets contained between half-multiples of $f_{\mathrm{rep}}^{(\mathrm{A})}$. Using the definition of $\Delta$, (1) can be recast to give an upper limit on $\Delta$ independent of $f_{\mathrm{rep}}^{(\mathrm{A})}$. The lower limit on $\Delta$ is given by the linewidth of the RF beats, requiring that the beats do not overlap one another. These limits are described in (2). For a fixed $\Delta$, the maximum optical bandwidth that can be sampled without aliasing is then given by (3):

$$\mathrm{LW_{RF}} < \Delta < \frac{f_{\mathrm{rep}}^{(\mathrm{B})} - 2N_H\,\delta_o}{2N_H\,(N_{\mathrm{B}} - 1) + 1}. \tag{2}$$

$$\mathrm{BW_{opt}} = \frac{f_{\mathrm{rep}}^{(\mathrm{A})} \cdot f_{\mathrm{rep}}^{(\mathrm{B})}}{2\Delta}. \tag{3}$$

The origin of each of the RF beat sets can be traced to distinct combline pairs in the optical domain. The first beat set, composed of beats between dc and $f_{\mathrm{rep}}^{(\mathrm{A})}/2$, arises from Comb B beating with the nearest lower frequency combline from Comb A. We shall call this the $\mathrm{Z}_{-1}$ beat set, where Z collectively refers to the complex amplitude of all beat tones in the set and $\mathrm{Z}(x)$ refers to the complex amplitude of the $x$th lowest frequency beat in that set. Similarly, the second beat set between $f_{\mathrm{rep}}^{(\mathrm{A})}/2$ and $f_{\mathrm{rep}}^{(\mathrm{A})}$ is a result of Comb B beating with the nearest higher frequency combline from Comb A, and we can thus designate the set as $\mathrm{Z}_{+1}$. This pattern continues, with the $\mathrm{Z}_{-2}$ ($\mathrm{Z}_{+2}$) set resulting from beats between Comb B and the second lowest (highest) frequency neighbors from Comb A. For a subharmonic order

of $N_H$, the first $N_H+1$ beat sets must be acquired to perform retrieval, setting a minimum required RF bandwidth as defined by (4). At large values of $N_H$, this is roughly equivalent to half of the larger repetition rate, $f_{\mathrm{rep}}^{(\mathrm{B})}$. This requirement, and the constraint it puts on the detection electronics, ultimately limits the maximum repetition rate comb that can be measured with multiheterodyne detection

$$\mathrm{BW_{RF}} \geq (N_H + 1)\,\frac{f_{\mathrm{rep}}^{(\mathrm{A})}}{2}. \tag{4}$$

### B. Amplitude and Phase Retrieval

Once a multiheterodyne signal satisfying the previous constraints has been obtained, the RF beat sets can then be manipulated to retrieve simultaneous, independent measurements of the spectral magnitude, and phase of each optical frequency comb. The essence of the retrieval algorithm is matching RF beat tones such that an optical combline common to both beats is canceled, giving the magnitude and phase relationship between adjacent comblines of a single comb [14]. In Fig. 1(a), three pairs of optical comblines are shown in stylized, colored arrows, with corresponding RF beats indicated in matching style and color in Fig. 1(b). In this simple example, it can be seen that the magnitude and phase relationship between comblines $\nu_5^{(\mathrm{A})}$ and $\nu_6^{(\mathrm{A})}$ can be determined independent of Comb B by taking the ratio of $\mathrm{Z}_{-3}(2)$ to $\mathrm{Z}_{-2}(2)$. The complex amplitude of combline $\nu_1^{(\mathrm{B})}$ drops out, yielding $\mathrm{A}_5/\mathrm{A}_6 \cdot e^{i(\alpha_6-\alpha_5)}$. Similarly, taking the ratio of $\mathrm{Z}_{-3}(2)$ to $\mathrm{Z}^*_{+2}(4)$ gives $\mathrm{B}_1/\mathrm{B}_0 \cdot e^{i(\beta_1-\beta_0)}$, independent of Comb A.

For a large number of comblines, the retrieval algorithm can be most easily visualized by first considering the negative half of the RF spectrum, where the negative frequency components are the complex conjugates of the positive components due to the photodetected intensity being a purely real signal. Shifting a copy of the RF spectrum by $f_{\mathrm{rep}}^{(\mathrm{A})}$ ($f_{\mathrm{rep}}^{(\mathrm{B})}$) and taking the ratio of overlapping beats then results in the adjacent combline relationships over the entire spectrum of Comb A (Comb B) [15]. This concept is illustrated in Fig. 2. At this point, the magnitude and phase of any one combline can be arbitrarily chosen, corresponding to a change of the waveform power and carrier-envelope phase offset, and the relative magnitude and phase of all other comblines can be calculated easily.

### C. Benefit of Subharmonic Multiheterodyne

The benefit of decreasing $f_{\mathrm{rep}}^{(\mathrm{A})}$ from nearly matched ($N_H = 1$) to a small subharmonic ($N_H \gg 1$) of $f_{\mathrm{rep}}^{(\mathrm{B})}$ is realized as a reduction in the RF bandwidth required to perform spectral retrieval. To demonstrate this, the maximum sampled optical bandwidth and the minimum required RF bandwidth as defined by (3) and (4) are plotted in Fig. 3 as functions of the effective repetition rate detuning. The detuning is normalized to units of $f_{\mathrm{rep}}^{(\mathrm{B})}$, which is held constant while $f_{\mathrm{rep}}^{(\mathrm{A})}$ is decreased to effect a change in $N_H$ and $\Delta$. In Fig. 3(a) and (b), it can be seen that both the optical bandwidth and the RF bandwidth decrease with larger $\Delta$, and both curves shift downward for increases in $N_H$.

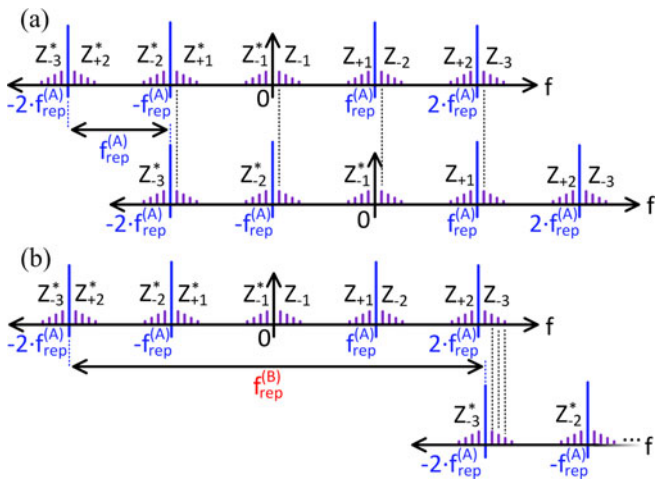


Fig. 2. Visual representation of retrieval algorithm for (a) low repetition rate Comb A and (b) high repetition rate Comb B.

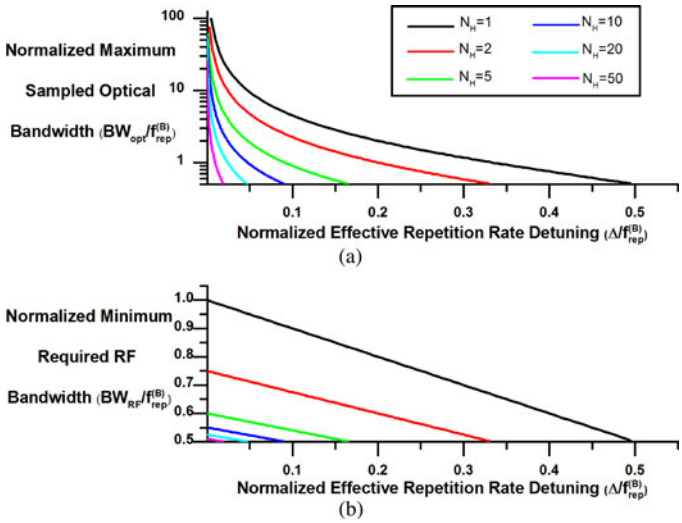


Fig. 3. Optical and RF bandwidth dependence on repetition rate detuning.

However, the region of large $N_H$ and small $\Delta$ can be exploited to achieve sampling of very large optical bandwidths using as little as $\frac{1}{2}\ f_{\mathrm{rep}}^{(\mathrm{B})}$ of RF bandwidth. Ultimately, the maximum optical bandwidth that can be sampled is determined by the minimum possible $\Delta$ [see (3)] which is in turn limited to the linewidth of the RF beats to avoid overlap. It should be noted that there exist digital postprocessing techniques to reduce the RF beat linewidth through phase estimation and frequency drift correction, which allow for reduction of $\Delta$ and an increase in optical bandwidth [16], [17].

### D. Description of Multiheterodyne Measurement

To perform each of the following experiments, the setup shown in Fig. 4 was used. A commercially available, carrier-envelope offset stabilized, mode-locked fiber laser with ~250 MHz repetition rate (OFC A) was beat against the ~10.25 GHz semiconductor laser under test (OFC B). A subharmonic order of 41 was achieved with these repetition rates, thus reducing the required RF bandwidth from ~10.25 to ~5.25 GHz

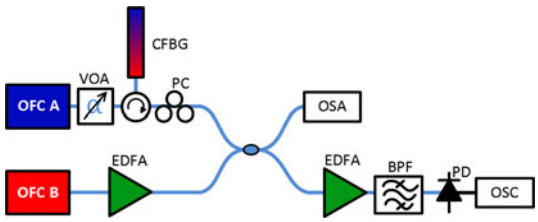


Fig. 4. Experimental setup. OFC, optical frequency comb; VOA, variable optical attenuator; PC, polarization controller; EDFA, erbium-doped fiber amplifier; BPF, bandpass filter; PD, photodetector; OSC, real-time oscilloscope; OSA, optical spectrum analyzer.

[see (4)]. This reduction in bandwidth was critical, enabling the multiheterodyne signal to be recorded with an 8 GHz bandwidth real-time oscilloscope and yielding the complex RF spectrum following a Fourier transform.

Oscilloscope traces lasting 20 $\mu$s are saved for offline postprocessing, though only $\sim$8 $\mu$s segments are used for calculation of the Fourier spectrum. This time duration is chosen to be equal to $N/\Delta$, where $N$ is an integer satisfying $N/\Delta < 1/\mathrm{LW_A}$. $\mathrm{LW_A}$ is the optical linewidth of one combline from OFC A, measured to be $\sim$100 kHz by a heterodyne measurement with a narrow linewidth continuous wave (CW) laser. As this linewidth is much broader than that of any of the 10.25 GHz test lasers, the maximum record length is effectively set by Comb A's coherence time to $\sim$10 $\mu$s. Thus, record lengths are chosen to be as long as possible to improve the signal-to-noise ratio (SNR), but less than the coherence time such that the entire signal is still coherent. Though not done here, phase noise compensation can be performed to increase record lengths and thus improve SNR [18].

One potential drawback of such a drastic difference in repetition rates is the increased power in the 250 MHz RF tone and its harmonics relative to an individual intercomb heterodyne beat. For every intercomb beat, there are 41 in-phase intracomb beats constructively contributing to the 250 MHz tone, resulting in it dominating the photodetected spectrum and the intercomb products being lost due to insufficient dynamic range. Equivalently, this can be interpreted in the time domain as the 250 MHz comb producing transform-limited pulses with high peak power relative to intercomb beat signals. To mitigate this effect, a chirped fiber Bragg grating (CFBG) was added to the optical path of the 250 MHz comb to effectively stretch the pulses to durations longer than the pulse period, creating a quasi-CW waveform and reducing power in the 250 MHz harmonics.

An example of multiheterodyne beat signal between the stretched 250 MHz comb output and the $\sim$10.25 GHz comb described in Section IV is shown in the oscilloscope trace in Fig. 5. A large dc background is present due to the quasi-CW pulsetrain, though some periodicity at 250 MHz can still be observed in the inset. The Fourier spectrum of this signal is shown in Fig. 6 in which distinct beat sets can be seen. The blue rectangle in Fig. 6 illustrates the spectrum used to perform retrieval for the 250 MHz comb, while the red rectangle contains the spectrum needed for retrieval of the 10.25 GHz comb. The portion in the red rectangle is expanded in the inset to show beat

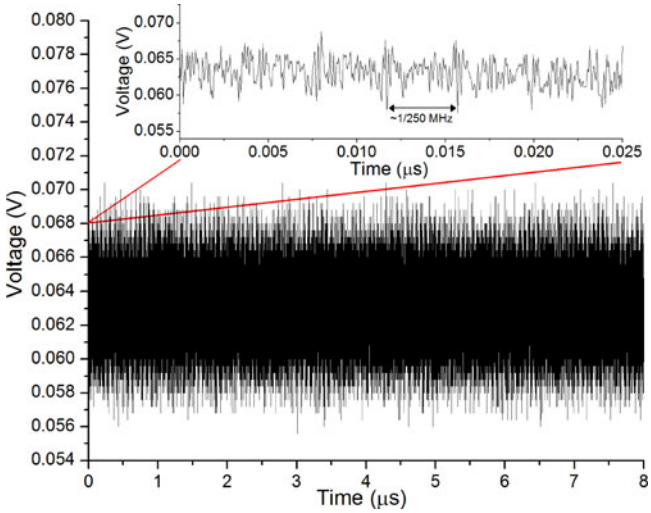


Fig. 5. Sample oscilloscope trace of multiheterodyne signal. Inset shows fast time-scale features, with clear periodicity from a 250 MHz comb source.

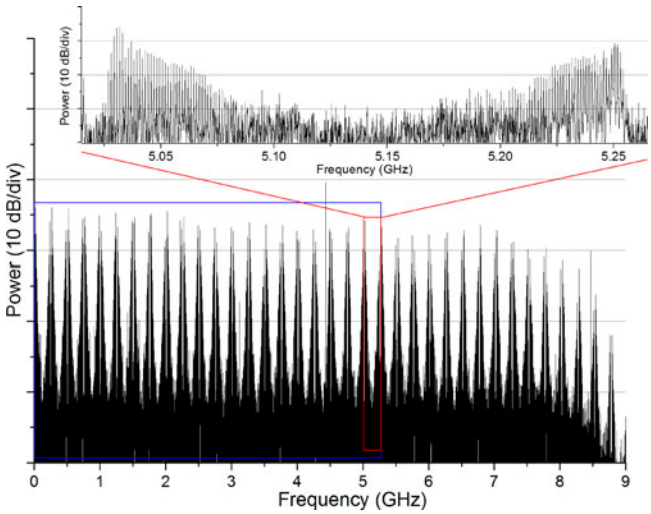


Fig. 6. Sample multiheterodyne Fourier spectrum. The blue rectangle highlights the portion of the spectrum required for magnitude and phase retrieval of 250 MHz comb. The red rectangle, expanded in inset to show beat set structure, indicates the spectral region required for magnitude and phase retrieval of 10.25 GHz comb.

set structure and individually resolvable combines with up to 30 dB SNR. It should be noted that balanced detection can be used to significantly improve the SNR [14], which was not done here due to lack of available detectors.

As a verification of the measurement technique, retrieval of the fiber laser's spectral phase yields a dispersion of $\sim$2046 ps/nm at 1550 nm, matching the specified dispersion of the CFBG which is the primary factor in shaping the phase of the otherwise transform-limited pulses. To quantify the higher order dispersion in each of the measured lasers, the retrieved phase was fit to the Taylor polynomial of

$$\Phi = \Phi_0 + \Phi_1 (\omega - \omega_o) + \frac{\Phi_2}{2!}(\omega - \omega_o)^2 + \frac{\Phi_3}{3!}(\omega - \omega_o)^3 . \quad (5)$$

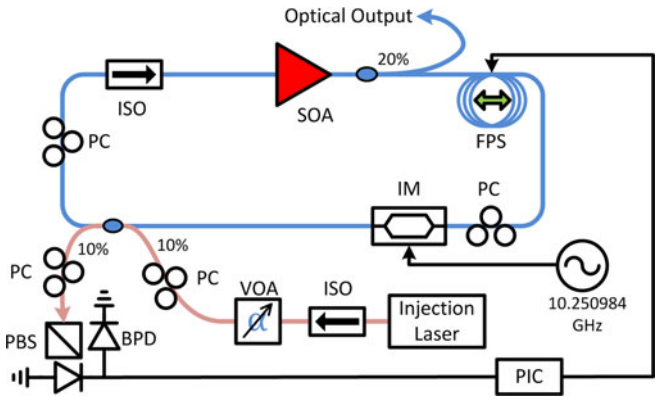


Fig. 7. Injection-locked harmonically MLL comb source. Slave optical cavity is shown in blue, with the injection arm and stabilization optics shown below it in red. PC, polarization controller; VOA, variable optical attenuator; ISO, optical isolator; PBS, fiberized polarization beam splitter.

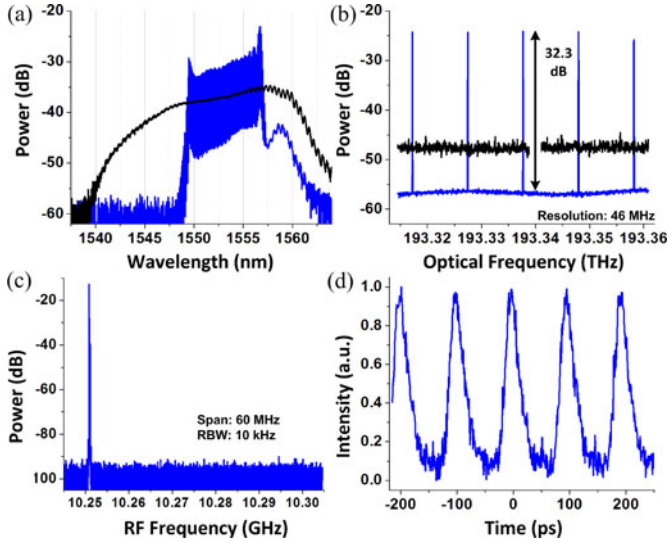


Fig. 8. (a) Output optical spectra and (b) high-resolution optical spectra of a harmonically MLL system with (blue) and without (black) injection locking. (c) RF spectrum of photodetected injection-locked comb source optical output. (d) Sampling oscilloscope trace of photodetected pulsetrain.

## III. Comb Generation Through Injection Locking of a Harmonically MLL

The first laser frequency comb source to be measured was an injection-locked harmonically MLL such as that of [19]. The laser, shown in Fig. 7, features a commercially available semiconductor optical amplifier (SOA) gain medium coupled into a long fiber cavity (4.26 m) for a cavity fundamental frequency of ∼47 MHz. The laser is harmonically mode locked via an intracavity Mach–Zehnder style intensity modulator (IM) at a rate of 10.250984 GHz, resulting in 218 pulses traversing the cavity simultaneously. The harmonically mode-locked spectrum typically consists of multiple groups of axial modes interleaved with an intragroup spacing at the repetition rate.

Generation of a frequency comb in such a spectrum can be achieved by selecting one of these phase correlated axial mode groups to exist. Other techniques, such as those in the following sections, utilize an intracavity etalon with free spectral range (FSR) equivalent to the mode-locking rate to suppress all other axial mode groups but one. In contrast, this laser uses single frequency injection into one cavity mode to generate the desired widely spaced frequency comb. The master injection laser is also a commercially available single frequency laser at 1550 nm. When injected into the laser cavity, injection locking of the selected cavity resonance is achieved, resulting in linewidth narrowing and frequency pulling to that of the master laser frequency. Energy is then shared via the mode-locking mechanism with other resonances of the same axial mode group at spacings of the repetition rate. Due to gain competition, other cavity resonances are suppressed, resulting in a high-quality frequency comb.

While the injection laser frequency remains within a "locking bandwidth" around the free-running slave laser resonance frequency, the laser will remain injection locked. Length fluctuations in the long fiber cavity due to environmental factors such as temperature and pressure will interrupt the injection-locked state, resulting in an unreliable source of optical frequency combs. Therefore, a scheme is necessary to detect these changes in cavity resonance frequency and feed back into the cavity to maintain the injection-locked state with high-quality comb output. To achieve this, a polarization spectroscopy technique first conceived by Hänsch and Couillaud [20] is utilized wherein orthogonal polarizations are interrogated in a polarization selective cavity. The scheme is shown in the bottom of Fig. 7. At the desired injection-locking frequency, one polarization is resonant while the orthogonal polarization is directly reflected, providing a convenient phase reference. At reflection, the two beams are projected onto one another again in a balanced photodetection scheme providing a voltage error signal, which is fed into a proportional-integrating controller to adjust an intracavity fiber phase shifter and affect the cavity resonance frequency.

The resulting optical spectra from the injection-locked frequency comb source are shown in Fig. 8(a) and a high-resolution spectrum is shown in Fig. 8(b). When no injection signal is present, the harmonically mode-locked spectrum appears continuous, due to the simultaneous lasing of the tightly spaced (47 MHz) laser cavity modes, below the resolution of both measurement devices. Injection-locked spectra, shown in blue, show a high-contrast 10.251-GHz-spaced optical frequency comb with ∼32 dB optical SNR, and 7.4 nm of bandwidth for a total of 90 comblines. Fig. 8(c) shows the photodetected RF spectrum of the laser, showing a strong RF tone at the mode-locking rate and large SNR and no RF supermode noise spurs (SNSs) visible above the noise floor over a large offset band. Ideal SNS suppression while maintaining reasonable injection-locked bandwidth was achieved with an injection power of 20 $\mu$W. A sampling oscilloscope trace can be seen in Fig. 8(d), clearly showing a ∼10.25 GHz pulsetrain.

An exceptional feature of this method of frequency comb generation is its versatility. The frequency comb spacing is determined by the mode-locking rate, which can be set to any multiple of the cavity fundamental frequency and finely tuned in

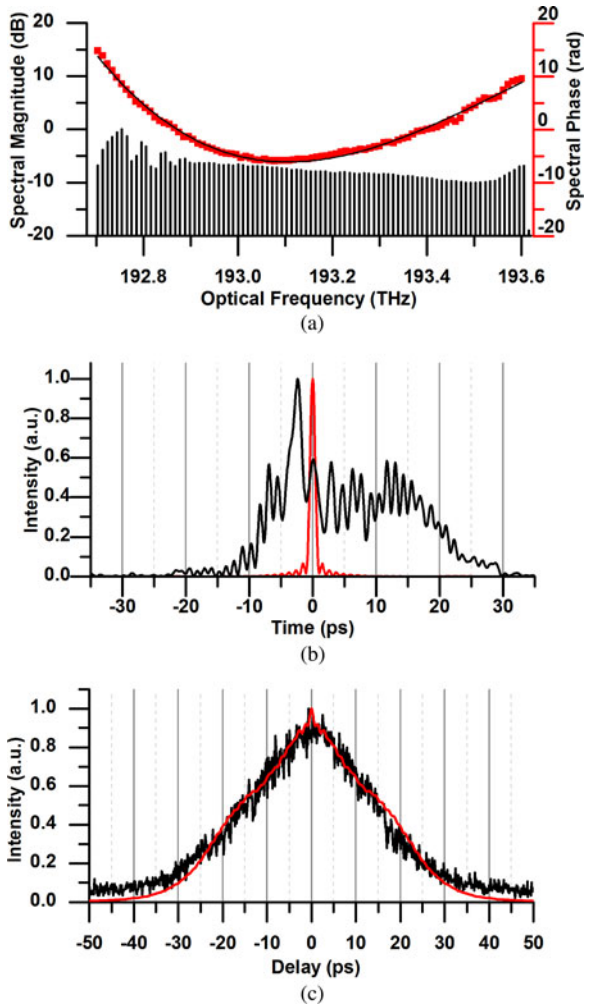


Fig. 9. (a) Measured spectral magnitude and retrieved phase. (b) Calculated pulse intensity profile (black) and transform-limited profile (red). (c) Comparison of calculated autocorrelation (red) and measured autocorrelation (black).

a smaller bandwidth as well. In addition, the absolute position of the comb can easily be shifted by adjusting the frequency of the optical injection signal. Therefore, the injection-locked laser comb source is an ideal source for use in multiheterodyne experiments with less versatile frequency comb sources since it effectively enables precise positioning of the entire RF spectrum via $\delta_o$, $\Delta$, and $N_H$.

In Fig. 9(a), the measured spectral intensity and the retrieved spectral phase can be seen, along with a fit of (5) to the spectral phase shown in black. From the fit parameters of the quadratic phase and cubic phase, we gain knowledge of the temporal pulse characteristics. The quadratic phase gives an estimate of the linear chirp or pulse broadening as compared to a perfectly transform-limited pulse, while the third-order phase coefficient provides a measure of the pulse asymmetry.

The polynomial fit yields values of 5.23 $ps^2$ and –1.59 $ps^3$ for the quadratic and cubic phase coefficients, respectively. From the quadratic phase coefficient, it is determined that the comb source produces down-chirped pulses with linear dispersion of 4.08 ps/nm at 1555 nm. The small, negative value of the third-order dispersion indicates the pulses are slightly asymmetric with temporal broadening on the trailing edge. In Fig. 9(b), the time-domain waveform as calculated from the measured spectrum and retrieved spectral phase of Fig. 9(a) is plotted. As predicted, the pulse has a sharp peak followed by a long tail at later times. Interestingly, there is a rapid modulation on top of the pulse with a period equal to the inverse of the spectral bandwidth. This is likely due to the sharp edges of the spectrum, as seen in Figs. 8(a) and 9(a).

A comparison of the autocorrelation calculated from the pulse in Fig. 9(b) and an experimentally measured autocorrelation is made in Fig. 9(c). Although the autocorrelation is an ambiguous measurement, the good agreement between the calculated and measured data suggests accurate retrieval from the multiheterodyne signal. It should be noted that the waveform and autocorrelation are calculated from the retrieved data, not the polynomial fit which is used solely to quantify the dispersion.

## IV. Comb Generation via a Coupled Cavity Approach

Low noise semiconductor-based harmonically MLLs have also been shown to produce a stable frequency comb using a cavity design that uses a long optical fiber cavity (∼28 m) coupled to a nested Fabry–Pérot Etalon (FPE) [21], [22]. In this architecture, narrow linewidth of the individual combline can be achieved due to the long storage time of the fiber cavity, which increases the cavity's frequency selectivity, and the wide mode spacing is imposed by the spacing of the transmission peaks of the transfer function of the FPE. The FPE thus serves the main purpose of selecting an axial mode group out of the $N$ possible ones from $N$th-order harmonic mode locking, as explained previously. In the time domain, the FPE can be understood as a storage element that correlates a pulse with $N$ other pulses, up to the decay time of the field in the cavity. If the fiber cavity length is chosen to be such that only one mode falls within the –3 dB bandwidth of the each of the etalon's transmission peaks (or, in the time domain, the fiber cavity is short enough that a pulse comes back to the etalon before its effects have decayed or become negligible), then a single pulse-train of nominally identical pulses with a well-defined (albeit sometimes unknown) carrier-envelope phase slip is generated and, in the frequency domain, this corresponds to a frequency comb.

The MLL experimental setup is shown in Fig. 10. A commercially available SOA is used for the experiments in this section and an optical cavity comprised of a single-mode fiber (SMF) is built around an FPE with a finesse of $10^3$. The laser is mode locked at 10.285324 GHz via loss modulation using an intracavity $LiNbO_3$ Mach–Zehnder electro-optic modulator. This modulator is driven by a radiofrequency synthesizer whose frequency is matched to the FSR of the FPE. Environmental drift makes it necessary to lock the fiber cavity to the FPE. This is achieved using a multicombline Pound–Drever–Hall (PDH) scheme, shown in the shaded box in Fig. 10. The PDH loop consists on phase modulating the output comb at 500 MHz and reinjecting this phase-modulated comb into the

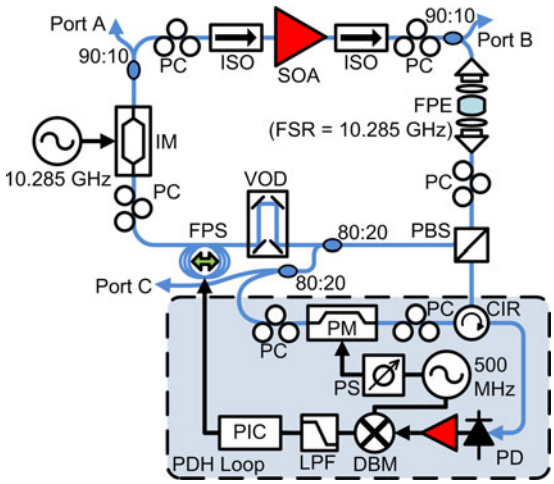


Fig. 10. Coupled cavity harmonically MLL comb source. VOD, variable optical delay; PM, phase modulator; CIR, circulator; DBM, double balanced mixer; LPF, low-pass filter; PS, phase shifter.

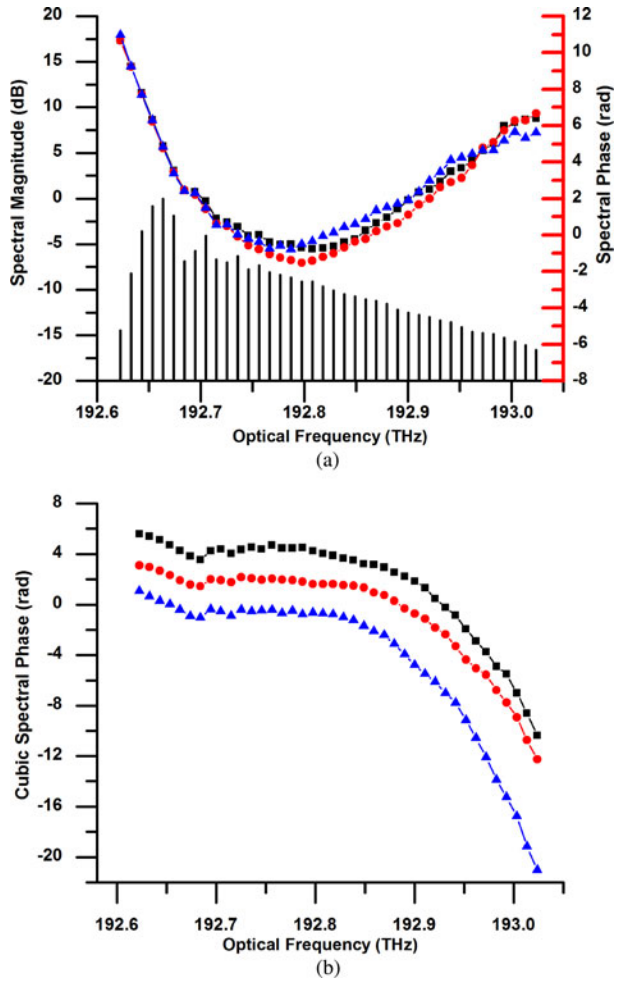


Fig. 11. (a) Measured spectral magnitude and retrieved phase from Port A (red circles), Port B (blue triangles), and Port C (black squares). (b) Residual cubic phase from each port, offset for clarity.

FPE in an orthogonal polarization state. The reflected sidebands are photodetected and mixed in quadrature with the 500 MHz tone to recover a signal that is proportional to the frequency difference between the transmission peaks of the FPE and the combines. This signal is then used to feed back to the fiber cavity length through a piezoelectric fiber stretcher. This loop essentially locks the fiber cavity fundamental frequency to a subharmonic of the FPE's FSR, or its optical path length to an integer multiple of the FPE's double-pass distance.

In order to analyze the evolution of the MLL pulses and spectrum around the cavity, we have built a cavity that has multiple output couplers (ports labeled A, B, and C) at different points, as shown in Fig. 10. In particular, we are interested in looking at spectral distortions that occur as the pulses go through the gain medium and the IM. Additionally, the filtering effect of the FPE can be observed by comparing ports B and C.

Fig. 11(a) shows a summary of the results for the retrieved spectral phase of the optical pulse at the three different ports as it propagates around the cavity. The salient features are somewhat similar to that obtained with the frequency comb source stabilized with injection-locking techniques in that the pulse in this case is also temporally broadened with linear down-chirp. However, the chirp is much larger than in the injection-locked case with an average quadratic phase of 16.18 $ps^2$ and a maximum of 17.12 $ps^2$ immediately after the SOA. This is equivalent to a dispersion of 16.18 ps/nm at 1555 nm. Exact values for the quadratic and cubic phase can be found in Table I.

The linear and quadratic spectral phase are removed in Fig. 11(b) to better examine changes in the third-order dispersion around the cavity. The relatively large cubic spectral phase suggests significant pulse asymmetry. More importantly, the cubic phase is nearly an order of magnitude larger than the injection-locked comb source, which is noteworthy given the fact that the etalon-based frequency comb laser is operating with approximately half the bandwidth of the injection-locked comb source. It should also be noted that the third-order phase is not affected by passage through the IM, as evidenced by the spectral phase from Port A being nearly identical to that from Port C. On the other hand, the spectral phase after the SOA gain element (Port B) does show a measurable difference suggesting that pulse shaping mechanisms are primarily dominated by the gain media. It is interesting to note the etalon acts as not just a spectral magnitude filter, but also as a spectral phase filter, reducing the amount of cubic phase from Ports B to C.

Pulse shapes calculated from the spectral information in Fig. 11 are shown in Fig. 12. For comparison, the theoretical transform-limited pulse produced by the spectral magnitude of Fig. 11(a) is also shown. In each case, the pulse consists of a sharp peak followed by a broad lobe with a long trailing edge. As in Fig. 9(b), rapid oscillations are observed atop the pulses, with period corresponding to the inverse of the spectral bandwidth. Due to the spectrum having smoother edges compared to that in Fig. 9(a), these oscillations are not as pronounced as those in Fig. 9(b). The calculated autocorrelations produced by these waveforms match well with the experimentally measured autocorrelations at each output port of the laser cavity.

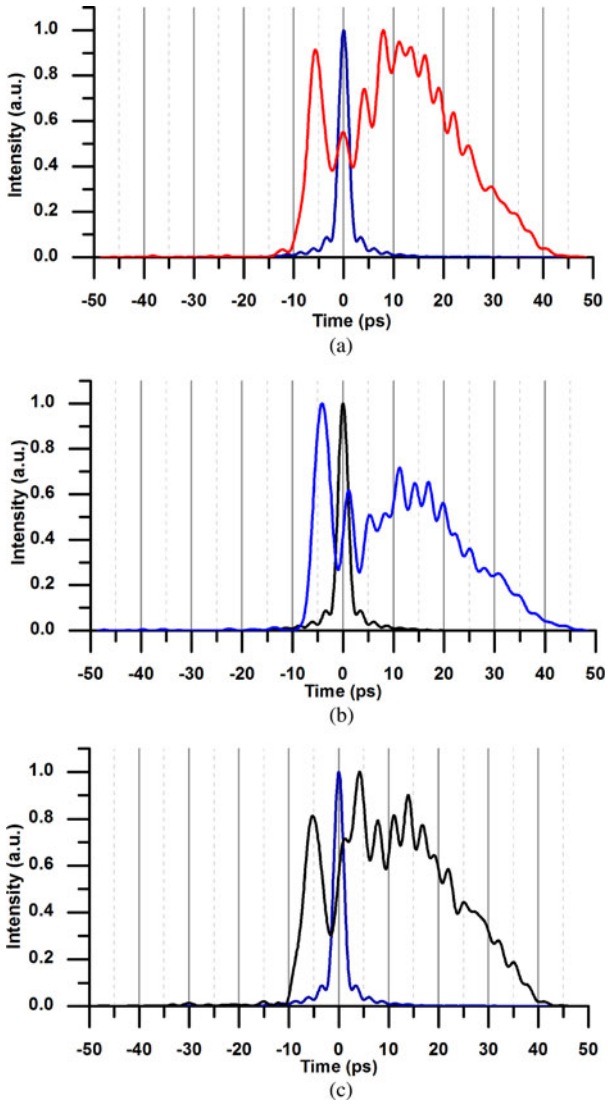


Fig. 12. Comparison of transform-limited pulses and retrieved time-domain waveforms from (a) Port A, (b) Port B, and (c) Port C.

## V. Dispersion Compensated Coupled Cavity Laser With a Slab-Coupled Optical Waveguide Amplifier (SCOWA)

A laser system similar to the one in the previous section was built separately, using an SCOWA as a gain medium. SCOWAs have a reduced confinement factor, significantly reducing beam intensity in the active region and thus reducing nonlinearity [23], [24]. This characteristic allows SCOWAs to achieve higher saturation power than standard waveguide SOAs with the tradeoff that the gain per unit length is lower. The reduced confinement factor also has the consequence that spontaneous emission is not efficiently coupled to the laser mode. In short, SCOWA devices have shown excellent performance with respect to saturation power, have a low noise figure, and have been used in ultralow noise MLLs and frequency combs [23], [24].

In this cavity (see Fig. 13), we have inserted a short section of a dispersion compensating fiber (DCF) in order to increase the mode-locked bandwidth. This allows for the generation of a considerably broader mode-locked spectrum. The output pulses

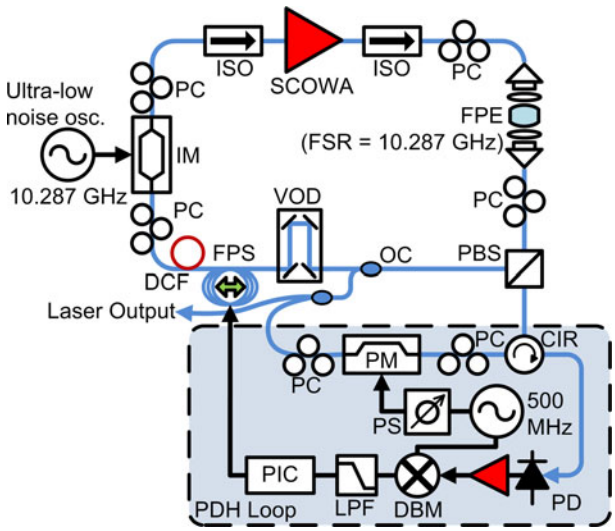


Fig. 13. Dispersion compensated coupled cavity harmonically MLL comb source.

have been shown to be compressible to near the Fourier transform limit [25]. The FPE used in this laser has also a finesse of ~1000, but its FSR is 10.287 GHz (detuned by ~2 MHz from the FPE in Section IV).

For the experiments presented here, we are aiming to extract fundamental information about the pulse shaping properties as the mode-locked frequency comb is passed through a second external SCOWA. The two initial conditions of importance to measure are the input comb with compressed pulses and with stretched pulses. To provide a clear understanding, five key spectra are measured: 1) direct laser output; 2) compressed output; 3) amplified output; 4) amplified and then compressed; and 5) compressed and then amplified. Cases 4 and 5 will shed insight into the role of nonlinear processes in the amplification of the mode-locked comb, since nonlinearities manifest themselves in reciprocal experiments resulting in nonreciprocal results. Results from amplification of short and long pulses are presented in Fig. 14.

In each of the spectra shown in Fig. 14, one will notice a distinct "lobe" at the high frequency end of the spectrum over which the phase is not retrieved. Due to a low SNR in the Fourier spectrum of the photodetected multiheterodyne signal, the large dip in the spectrum preceding the lobe falls below the measurement noise floor, effectively isolating the lobe from the rest of the spectrum. Though theoretically possible, current implementation of the phase retrieval algorithm is incapable of handling such spectral holes. Accurate prediction of the expected intensity or autocorrelation shapes for these measurements is thus precluded, as there is significant power contained in this lobe over which the phase is not retrieved.

Fig. 14(a) shows the measured spectral intensity of the stabilized comb pulsetrain directly from the output of the laser, along with the retrieved spectral phase. It is recognized immediately that the fundamental shape of the retrieved phase is different in that the sign of both quadratic and cubic phase is opposite of that of the previous two comb sources. Hence, the pulses from

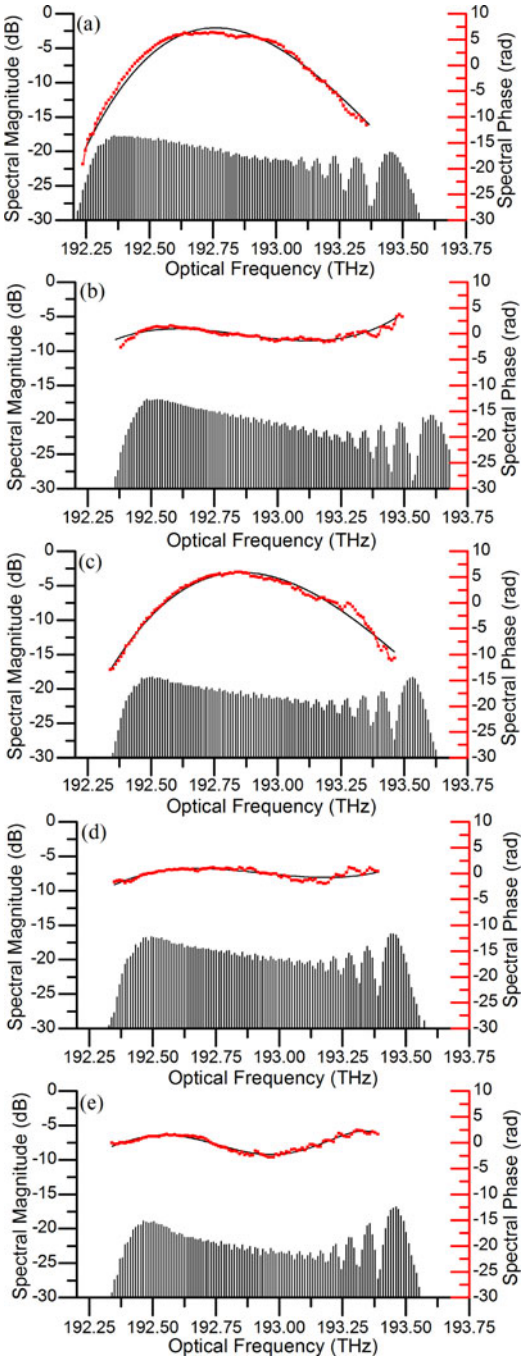


Fig. 14. Spectra with retrieved phase for (a) directly from laser, (b) compression with an SMF, (c) external SCOW amplification, (d) amplification then compression, and (e) compression then amplification.

this dispersion compensated cavity are up-chirped and mildly asymmetric with a longer leading edge. This sign change can be attributed to the inclusion of the normally dispersive DCF. It should also be noted that the magnitude of both second- and third-order phase is substantially reduced as compared to the other sources, likely due to both successful dispersion balancing with the DCF and less nonlinearity in the gain from a lower mode confinement factor in the SCOWA. Numerical values for the quadratic and cubic phase from all measurement cases can be found in Table I.

Compression of the optical pulses was achieved by passing the pulse train through 130 m of an SMF to compensate for the quadratic phase. The resulting spectral phase shown in Fig. 14(b) suggests that the quadratic component has been significantly reduced, leaving residual third-order phase of similar magnitude as that directly from the laser.

The primary feature of interest from the measurement of the spectral phase after external SCOW amplification [see Fig. 14(c)] is the small, but meaningful reduction in both quadratic and cubic phase. While the quadratic phase reduction can be attributed to extra fiber path length from pigtails, the cubic reduction is likely due to the SCOWA itself. Notice that the SCOWA adds a negative contribution to the cubic phase, similar to the effect of the SOA in the nondispersion compensated cavity between ports A and B, but the magnitude of the contribution is much less, possibly because of the lower mode confinement factor.

In Fig. 14(d), the amplified pulsetrain from the previous measurement was passed through the 130 m of an SMF. In this case, we observed the quadratic phase to be similar to that from just compression [see Fig. 14(b)] and the cubic phase to be similar to that from just amplification [see Fig. 14(c)]. This appears to be an effective amplification scheme for obtaining high peak powers, as it results in the lowest overall nonlinear phase and is therefore theoretically the most compressible.

Finally, the pulses were first compressed in the 130 m of an SMF and then amplified with the SCOWA. As can be seen in Fig. 14(e), this resulted in a significant distortion of the spectral phase. No longer well described by a third-order polynomial, this phase profile was fit to a fifth-order Taylor expansion. The parameters in Table I from the fifth-order fit indicate a substantial positive increase in the cubic phase. While this value is questionable, the important characteristic of this measurement is the clear, dramatic change in the phase profile, making these pulses difficult to further compress without more advanced techniques.

## VI. Conclusion

The results from each multiheterodyne characterization are summarized in Table I. As can be seen from the first two comb sources, in the absence of the DCF in the laser cavity, the spectral phase has a positive quadratic component and negative cubic component, leading to the pulses being down-chirped and asymmetric with a long trailing edge. The larger magnitude phase coefficients of the FPE-stabilized MLL as compared to the injection-locked MLL are likely due to the substantially longer fiber cavity length, increasing the total cavity dispersion. Comparing ports A to B of the FPE stabilized source, it can be seen that the standard waveguide SOA contributes significant negative third-order phase to the spectral phase profile. The intracavity FPE is seen to filter and reduce the magnitude of the cubic phase between ports B and C. This effect may be caused by the phase response across an etalon resonance, described by an odd function, acting to balance the cubic phase as laser modes walk off from resonance center.

In contrast to the first two comb sources, the SCOWA-based dispersion compensated MLL produces slightly asymmetric

TABLE I
SUMMARY OF SECOND- AND THIRD-ORDER PHASE COEFFICIENTS

| Comb Source | Measurement (Figure) | $\Phi_2$ ($ps^2$) | D (ps/nm) | $\Phi_3$ ($ps^3$) |
|---|---|---|---|---|
| Injection locked MLL | Inj. Lock (7a) | 5.23 | 4.08 | -1.59 |
| FPE stabilized MLL | Port A (9) | 20.52 | 15.99 | -15.13 |
| | Port B (9) | 21.96 | 17.12 | -21.32 |
| | Port C (9) | 19.80 | 15.43 | -15.57 |
| High power and dispersion compensated FPE stabilized MLL | Direct (12a) | -3.79 | -2.95 | 0.82 |
| | Compressed (12b) | -0.84 | -0.65 | 0.80 |
| | Amplified (12c) | -3.13 | -2.44 | 0.61 |
| | Amp. & Comp. (12d) | -0.42 | -0.33 | 0.64 |
| | Comp. & Amp.* (12e) | -0.17 | -0.13 | 2.83 |

*The values for the compressed and amplified results are obtained from a fifth-order fit, as opposed to third for all others.

up-chirped pulses with a longer leading edge largely due to the negative dispersion and negative dispersion slope of the DCF. The dispersion compensation, along with the low-dispersion gain, results in smaller magnitude phase coefficients than either of the other sources, making the pulses compressible to near Fourier transform limited in 130 m of an SMF. Considering the difference between the directly measured output and the externally amplified, the SCOWA is determined to add negative cubic phase, similar to the standard SOA, but an order of magnitude less. The reduction in magnitude is attributed to less nonlinearity in the gain due to a lower confinement factor. Amplification of compressed pulses is shown to increase nonlinearity in the gain and cause distortion of the spectral phase.

In conclusion, we have presented a multiheterodyne measurement technique for the characterization of spectral phase, independent of reference comb source. We applied this technique to three different semiconductor-based optical frequency combs and measured the amount of quadratic and cubic phase in each. The measured phase coefficients were then traced back to effects in the semiconductor gain, fiber cavity, and FPE. With this knowledge, we can hope to more efficiently balance the dispersion of these laser cavities and increase their spectral bandwidth.

## REFERENCES


[1] T. Udem, R. Holzwarth, and T. W. Hansch, "Optical frequency metrology," *Nature*, vol. 416, no. 6877, pp. 233–237, Mar. 2002.

[2] J. Ye, J.-L. Peng, R. J. Jones, K. W. Holman, J. L. Hall, D. J. Jones, S. A. Diddams, J. Kitching, S. Bize, J. C. Bergquist, L. W. Hollberg, L. Robertsson, and L.-S. Ma, "Delivery of high-stability optical and microwave frequency standards over an optical fiber network," *J. Opt. Soc. Amer. B*, vol. 20, no. 7, pp. 1459–1467, Jul. 2003.

[3] A. M. Weiner, "Femtosecond pulse shaping using spatial light modulators," *Rev. Sci. Instrum.*, vol. 71, no. 5, pp. 1929–1960, May 2000.

[4] P. J. Delfyett, I. Ozdur, N. Hoghooghi, M. Akbulut, J. Davila-Rodriguez, and S. Bhooplapur, "Advanced ultrafast technologies based on optical frequency combs," *IEEE J. Sel. Topics Quantum Electron.*, vol. 18, no. 1, pp. 258–274, Jan./Feb. 2012.

[5] P. J. Delfyett, S. Gee, M. T. Choi, H. Izadpanah, W. Lee, S. Ozharar, F. Quinlan, and T. Yilmaz, "Optical frequency combs from semiconductor lasers and applications in ultrawideband signal processing and communications," *J. Lightw. Technol.*, vol. 24, no. 7, pp. 2701–2719, Jul. 2006.

[6] T. J. Kippenberg, R. Holzwarth, and S. A. Diddams, "Microresonator-based optical frequency combs," *Science*, vol. 332, no. 6029, pp. 555–559, Apr. 2011.

[7] R. Trebino, *Frequency-Resolved Optical Gating: The Measurement of Ultrashort Laser Pulses*. New York: Springer, 2000.

[8] C. Iaconis and I. A. Walmsley, "Spectral phase interferometry for direct electric-field reconstruction of ultrashort optical pulses," *Opt. Lett.*, vol. 23, no. 10, pp. 792–794, May 1998.

[9] F. Ferdous, D. E. Leaird, C. B. Huang, and A. M. Weiner, "Dual-comb electric-field cross-correlation technique for optical arbitrary waveform characterization," *Opt. Lett.*, vol. 34, no. 24, pp. 3875–3877, Dec. 2009.

[10] J. Davila-Rodriguez, M. Bagnell, C. Williams, and P. J. Delfyett, "Multiheterodyne detection for spectral compression and downconversion of arbitrary periodic optical signals," *J. Lightw. Technol.*, vol. 29, no. 20, pp. 3091–3098, Oct. 2011.

[11] S. Schiller, "Spectrometry with frequency combs," *Opt. Lett.*, vol. 27, no. 9, pp. 766–768, May 2002.

[12] I. Coddington, W. C. Swann, and N. R. Newbury, "Coherent multiheterodyne spectroscopy using stabilized optical frequency combs," *Phys. Rev. Lett.*, vol. 100, no. 1, pp. 013902-1–013902-4, Jan. 2008.

[13] I. Coddington, W. C. Swann, and N. R. Newbury, "Coherent dual-comb spectroscopy at high signal-to-noise ratio," *Phys. Rev. A*, vol. 82, no. 4, pp. 043817-1–043817-13, Oct. 2010.

[14] N. K. Fontaine, D. J. Geisler, R. P. Scott, and S. J. B. Yoo, "Simultaneous and self-referenced amplitude and phase measurement of two frequency combs using multi-heterodyne spectroscopy," in *Proc. Opt. Fiber Commun. Conf.*, Mar. 2012, pp. 1–3, Paper OW1C.1.

[15] A. Klee, J. Davila-Rodriguez, M. Bagnell, and P. J. Delfyett, "Self-referenced spectral phase retrieval of dissimilar optical frequency combs via multiheterodyne detection," in *Proc. IEEE Photon. Conf.*, Sep. 2012, pp. 1–2, Paper WI2.

[16] P. Giaccari, J. D. Deschenes, P. Saucier, J. Genest, and P. Tremblay, "Active Fourier-transform spectroscopy combining the direct RF beating of two fiber-based mode-locked lasers with a novel referencing method," *Opt. Exp.*, vol. 16, no. 6, pp. 4347–4365, Mar. 2008.

[17] M. G. Taylor, "Phase estimation methods for optical coherent detection using digital signal processing," *J. Lightw. Technol.*, vol. 27, no. 5–8, pp. 901–914, Apr. 2009.

[18] G. H. Liu and W. L. Zhu, "Compensation of phase noise in OFDM systems using an ICI reduction scheme," *IEEE Trans. Broadcast.*, vol. 50, no. 4, pp. 399–407, Dec. 2004.

[19] C. Williams, J. Davila-Rodriguez, K. Bagnell, and P. J. Delfyett, "Stabilization of an injection locked harmonically mode-locked laser via polarization spectroscopy for frequency comb generation," in *Proc. Lasers Electro-Opt. Conf. Quantum Electron. Laser Sci.*, May 2012, pp. 1–2, Paper JTH2A.50.

[20] T. W. Hansch and B. Couillaud, "Laser frequency stabilization by polarization spectroscopy of a reflecting reference cavity," *Opt. Commun.*, vol. 35, no. 3, pp. 441–444, Dec. 1980.

[21] F. Quinlan, C. Williams, S. Ozharar, S. Gee, and P. J. Delfyett, "Self-stabilization of the optical frequencies and the pulse repetition rate in a coupled optoelectronic oscillator," *J. Lightw. Technol.*, vol. 26, no. 13–16, pp. 2571–2577, Aug. 2008.

[22] I. Ozdur, M. Akbulut, N. Hoghooghi, D. Mandridis, S. Ozharar, F. Quinlan, and P. J. Delfyett, "A semiconductor-based 10-GHz optical comb source with sub 3-fs shot-noise-limited timing jitter and similar to 500-Hz comb linewidth," *IEEE Photon. Technol. Lett.*, vol. 22, no. 6, pp. 431–433, Mar. 2010.

[23] W. Loh, J. J. Plant, J. Klamkin, J. P. Donnelly, F. J. O'Donnell, R. J. Ram, and P. W. Juodawlkis, "Noise figure of watt-class ultralow-confinement semiconductor optical amplifiers," *IEEE J. Quantum Electron.*, vol. 47, no. 1, pp. 66–75, Jan. 2011.

[24] P. W. Juodawlkis, J. J. Plant, R. K. Huang, L. J. Missaggia, and J. P. Donnelly, "High-power 1.5-mm InGaAsP-InP slab-coupled optical waveguide amplifier," *IEEE Photon. Technol. Lett.*, vol. 17, no. 2, pp. 279–281, Feb. 2005.

[25] J. Davila-Rodriguez, I. Ozdur, M. Bagnell, P. Delfyett, J. Plant, and P. Juodawlkis, "Ultralow noise, etalon stabilized, 10 GHz optical frequency comb based on a SCOW amplifier," *IEEE Photon. Technol. Lett.*, vol. 24, no. 23, pp. 2159–2162, Dec. 2012.



**Anthony Klee** (S'11) received the B.S. degree in optical engineering from the Rose-Hulman Institute of Technology, Terre Haute, IN, in 2010, and the M.S. degree in optics from the University of Central Florida, Orlando, in 2013, where he is currently working toward the Ph.D. degree in optics at the Center for Research and Education in Optics and Lasers.

His research interests include generation of optical frequency combs from semiconductor mode-locked lasers and the development of novel measurement techniques for the characterization of these combs.

Mr. Klee is a student member of the IEEE Photonics Society.

**Josue Davila-Rodriguez** (S'11) received the B.S. degree in engineering physics from the Tecnologico de Monterrey, Monterrey, Mexico, in 2006. He is currently working toward the Ph.D. degree at the University of Central Florida, Orlando.

He joined the Center for Research and Education in Optics and Lasers, University of Central Florida in 2007. His research interests include novel mode-locked laser sources and their applications.

**Charles Williams** (S'06) received the B.S. degree in physics from the University of Missouri–Rolla, Rolla, in 2006, the M.S. degree in optics from the University of Central Florida, Orlando, in 2008, where he is currently working toward the Ph.D. degree in optics.

He is currently a Graduate Student with the Center for Research and Education in Optics and Lasers and the Florida Photonics Center of Excellence, College of Optics and Photonics, University of Central Florida. His research interests include the creation of low-noise oscillators and optical comb sources for communications, laser ranging, and signal processing—namely through the use of injection-locking techniques.

Mr. Williams is a student member of the IEEE Photonics Society.

**Peter J. Delfyett** (S'79–M'94–SM'96–F'02) received the Ph.D. degree in electrical engineering from the City University of New York, New York, in 1988.

From 1988 to 1993, he was a member of the Technical Staff with Bell Communications Research. He is the University of Central Florida Trustee Chair Professor of optics, electrical engineering, and physics at the College of Optics and Photonics and the Center for Research and Education in Optics and Lasers. He has published more than 650 articles in refered journals and conference proceedings, and has been awarded 35 US Patents.

Dr. Delfyett served as the Editor-in-Chief of the IEEE JOURNAL OF SELECTED TOPICS IN QUANTUM ELECTRONICS (2001–2006), and served on the Board of Directors of the Optical Society of America. He served as the Associate Editor of IEEE PHOTONICS TECHNOLOGY LETTERS, and was the Executive Editor of the IEEE Photonics Society (1995–2000). He is a Fellow of the Optical Society of America, IEEE Photonics Society, and American Physical Society. He was also a member of the Board of Governors of the IEEE Photonics Society (2000–2002) and a member of the Board of Directors of the Optical Society of America (2004–2008). In addition, he received the National Science Foundation's Presidential Faculty Fellow Early Career Award for Scientists and Engineers, which is awarded to the Nation's top 20 young scientists. He received the University of Central Florida's 2001 Pegasus Professor Award which is the highest honor awarded by the University. He has also endeavored to transfer technology to the private sector, and helped to found "Raydiance, Inc." which is a spin-off company developing high power, ultrafast laser systems, based on his research, for applications in medicine, defense, material processing, biotech, and other key technological markets. Most recently, he received the APS Edward Bouchet Award for his significant scientific contributions in the area of ultrafast optical device physics and semiconductor diode-based ultrafast lasers, and for his exemplary and continuing efforts in the career development of underrepresented minorities in science and engineering.